Ecole Polytechnique de Lausanne
Politecnico di Torino

Tenth International Symposium on Magnetic Bearings

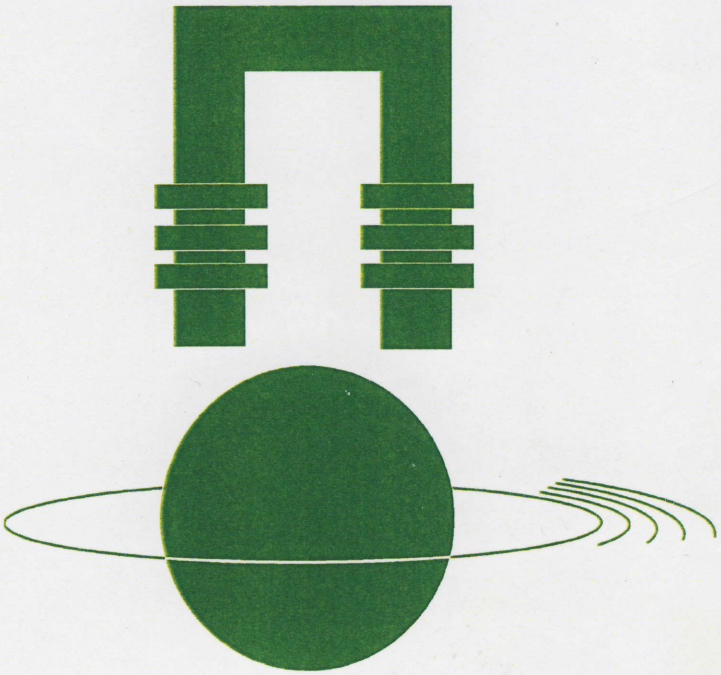

Abstracts

Edited by:
Hannes Bleuler
Giancarlo Genta

August 21-23, 2006, Martigny Switzerland

Analysis of Bearingless Motor with Rectifier Circuits*

Chen Li, Hironobu Aratani, and Koichi Oka

Dept. of Intelligent Mechanical System Engineering
Kochi University of Technology,
Kochi-Pref, 782-8502, Japan
Oka.koichi@kochi-tech.ac.jp

***Abstract* – In this paper, feasibility studies for a new type of bearingless motor are carried out by FEM analyses and experiments. The feature of the bearingless motor is using a rotor with rectifier circuit coil, which makes the rotor act as a permanent magnet. The optimum geometrical dimensions of the proposed bearingless motor are determined by the calculations of rotor torques about various rotor tooth lengths. The results indicate that large enough torque can be generated. The dimension with which the motor has relatively minimum fluctuation and smoothness torque has been chosen to build a test model. In order to realize the radial forces and rotation control, a strategy which adopts sine and cosine control currents of rotor angle has been test. FEM analysis is also used for evaluating the property of the proposed strategy. The results show that the generated radial force fluctuates with the rotor angle, however, the linearity of the generated forces to control currents is verified, and feedback control can be used to reduce this problem.**

***Index terms* – bearingless motor, rectifier circuits, control current arrangement, FEM analysis**

I. INTRODUCTION

Bearingless motor possesses the capabilities of both a magnetic bearing and a motor. It is therefore able to suspend the rotor and generate torque simultaneously. It is also called self-bearing motor or integrated motor bearing. The main challenge in this technology lies in the design of a control device and algorithm that coordinates the radial forces without interfering with the function of the motor. Bearingless motor has not only the advantages of magnetic bearing, such as negligible friction loss, no wear, high reliability, low-maintenance, and higher speeds for extreme environments in no need of complex lubrication systems, but also has a shorter shaft compared with the conventional motor and magnetic bearing. Thus, the critical rotating speed can be increased. Bearingless motors can be used at some special fields such as biomedical products, e.g. artificial heart; it also can be used as high speed drives and generators.

Since bearingless motors have so many advantages and special applications, so far, various types of bearingless motors have been developed. As far as the stator winding configuration is concerned, a representative one is the 4 poles motor winding and 2 poles radial force winding structure, regulating the air gap flux distribution to generate a radial force in any desired directions [1]-[5].

From the point of view of motor types, permanent bearingless motor is widely developed. Compared with the electromagnetic motor, permanent bearingless motor is more effective even with a relatively large air gap; it is helpful to reduce the motor volume using permanent magnet. However, for permanent magnet, there are also some disadvantages, such as demagnetization and limited mechanical strength [6].

In [7], another type of bearingless motor has been proposed. The feature of the proposed motor is that there is a rectifier circuit in the rotor winding. The feasibility analysis had been carried out by means of simple numerical simulation. Compared with the permanent magnet bearingless motors, the proposed bearingless motor possesses such advantages as no demagnetization, much less rotor reluctance and being liable to realize serial production. In this paper, further study results are presented, FEM analysis and experimental results show that this structure can be put into practice.

II. PRINCIPLE OF THE PROPOSED BEARINGLESS MOTOR

The configuration schematic of rectified bearingless motor is shown in Fig.1. It has a four poles rotor and eight poles stator. Details of corresponding one set of rotor, stator and coils are illustrated in Fig.2. In the figure, it can be seen that there are two sets of coils on the stator poles. One set of coil is connected with the opposing stator coil in series. This coil is excited by AC current, and it is called exciting coil. The control currents are applied to the other

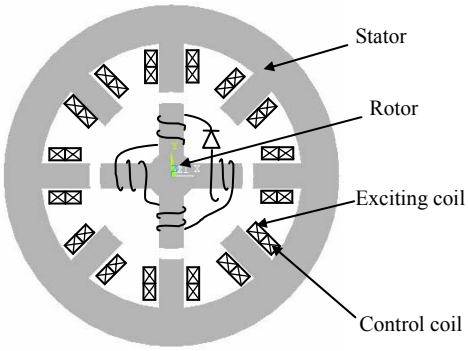

Fig.1 The schematic of rectified bearingless motor

* This work is partially supported by Grant-in-Aid for Scientific Research to K. Oka.

set of coil to control the rotor torque and radial force, these coils called control coil.

In addition, one set of coils is wound on the rotor poles in series, and a rectifier diode is joined to the rotor winding circuits. When AC current is applied to the exciting coil, DC current will be induced in the rotor windings owing to the existence of the rectifier diode, therefore the rotor possesses fixed polarity poles and works just like a permanent magnet.

Fig.3 shows the simulation results of exciting voltage, induced rotor current and rotor flux. It can be seen that when AC current is applied to the exciting coil, DC current is induced in the rotor coil, and the rotor flux almost keeps constant. These results indicate that the rotor is able to act as a permanent magnet.

The experimental results of radial force with respect to control current are given in Fig.4. This figure shows the comparison of the radial force with and without exciting current. When the exciting voltage is zero, the radial force keeps a fixed direction with changing the amplitude and

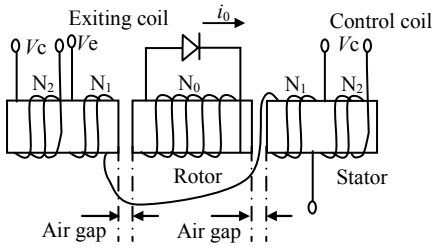

Fig.2 The schematic of rectified rotor and stator

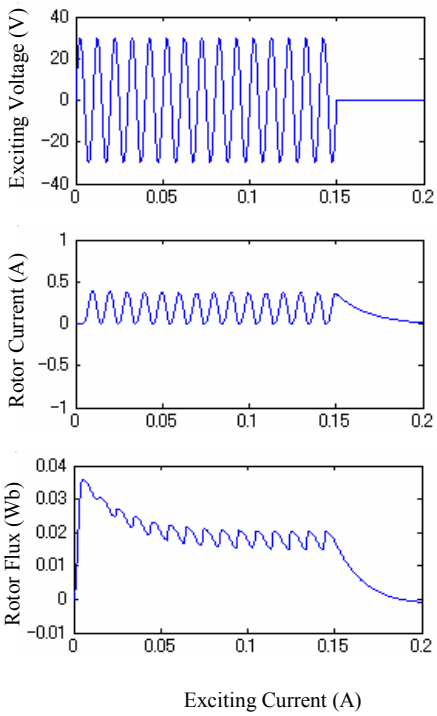

Fig.3 Simulation results of exciting voltage, rotor current and flux

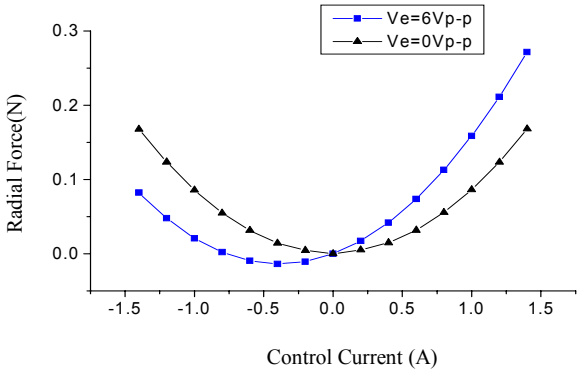

Fig.4 Experimental results of radial force versus control current

direction of control current. However, when the exciting voltage is 6 volts, negative forces can be generated as regulating the amplitude and direction of control current. It is further indicated that the existence of rectified coil makes the rotor possess fixed polarity and have the characteristic of a permanent magnet.

In fact, the rotor is made of silicon iron, whose reluctance is much less than permanent magnet reluctance and the demagnetization will not be caused. Adjusting the magnitude and directions of control current can control the radial force and rotation torque, and the motor can work just like a permanent magnet stepping motor.

III. THE PROTOTYPE DESIGN AND ANALYSIS

A. The improvement of test model

At first, a series of FEM calculation and experiments have been carried out with the test model shown in Fig.1. The experimental results show that the radial force is insufficient to levitate the rotor, and there exists zero torque position when the rotor and stator poles are aligned with each other. These results can be explained by the flux distribution shown by Fig.5. It can be seen that only few of flux lines flow between the rotor and adjacent stator tooth. It is caused by the large air gap between the rotor and adjacent stator tooth.

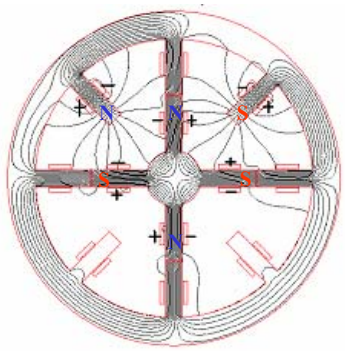

Fig.5 Flux distribution of old model

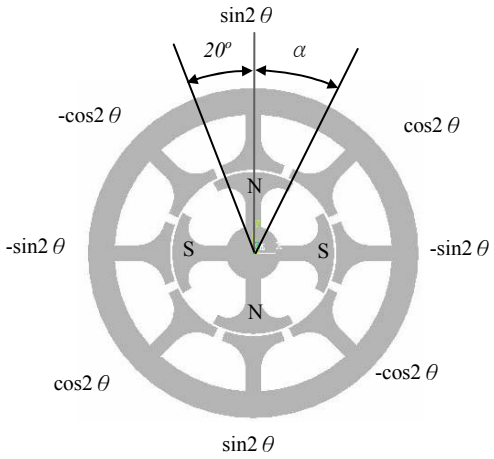

Fig.6 New shape of bearingless motor

A new prototype bearingless motor is designed. The new shape of the bearingless motor is schematically shown in Fig.6. The coils wound on the rotor and stator poles are identical to those demonstrated in Fig.1. Since the shape of rectifier bearingless motor has been determined, an optimum dimension of the bearingless motor is desired, so that a relatively large radial force and torque can be generated.

Based on the assumption that the rotor is located at the geometrical centre of the motor, and it is magnetized by uniform induced current, a series of analyses have been carried out by FEM to determine the dimension best suitable for the bearingless motor with rectifier circuits. Firstly, the motor radius and length of stator tooth surface have been determined, the optimum length of rotor tooth is what we desire to know. In Fig.6, the radius of the rotor is 60mm, and the angle of the stator tooth is 40 degrees.

In order to rotate the rotors, the sine and cosine control current arrangement of rotation angle is applied as shown in Fig.6. In the figure, θ is the rotational angle of the rotor which rotates in counterclockwise, the rotor position in Fig.6 is corresponding to the starting angle 0^o. α is the angle of front edge of rotor tooth with respect to the vertical line. The torques at various rotor angular positions have been calculated when α changes from 15^o to 40^o, with the incremental angle being 5 degrees. These variations of α corresponding the length of rotor tooth is shorter, equal or longer compared with the stator tooth length. Fig.7 gives the flux distribution corresponding α is equal to 30 degree. It can been seen that much more flux lines flow between the stator and adjacent rotor tooth. Because of the symmetry configuration of the rotor and the stator, the rotor angle θ changes from 0^o to 90^o. The results of torque are given in Fig.8.

From Fig.8 it can be seen that with the increasing of the rotor tooth length, the curves of torques become flat. It can be found that a relatively large and smooth torque can be obtained when the angle α is equal to 30 degree, so this dimension has been chosen for the new bearingless motor prototype.

From Fig.8, it can also be seen that the torque approaches its maximum when the rotor polar front edge begins to align with the stator tooth face about all α. For example, when α is equal to 15^o, and the rotor angle position θ is 10^o, the torque reaches its maximum when the rotor poles front edge begins to overlap with the next stator tooth face.

For the new test model, when the control currents shown in Fig.6 are applied to the control coil, the corresponding radial forces have also been calculated.

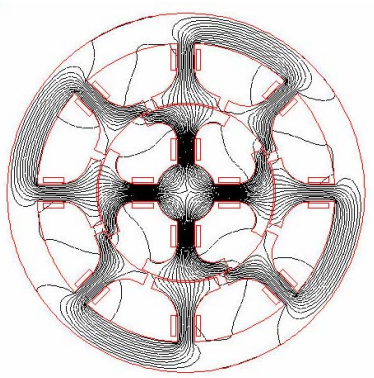

Fig.7 Flux distribution of α equal to 30 degrees

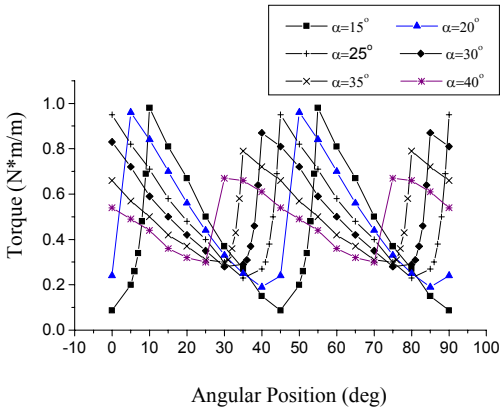

Fig.8 Torques for different rotor dimensions

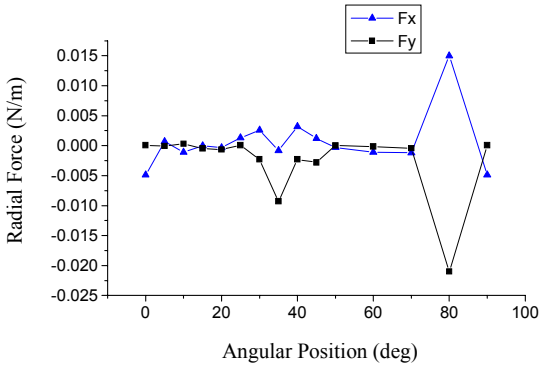

Fig.9 Radial force corresponding to α of 30 degree

Fig.9 presents the results of radial forces versus the rotor angular positions. From this figure, it can be concluded that the radial force is very small and can be neglected, therefore this control current arrangement of rotor rotation will not interfere with the rotor radial force function.

The performance of new prototype model has been compared with the old one. When same control currents shown in Fig.5 are applied to the new model, the comparison results are shown in Fig.10 and Fig.11. It can be seen that there are much larger radial force and torque can be generated in the new test model, and there is no zero torque position.

B. No interfering of superimposed DC Current with the motor function

For bearingless motor, the major challenge lies in the design of a control device and algorithm which can control the radial forces without interfering with the function of the motor. According to the assumption mentioned above, the radial forces and torques are adjusted by control current. In order to investigate the effects of control currents will generate, based on the control current arrangement shown in Fig.6, a constant value β is superimposed upon the control current of the top stator pole and - β to the opposing stator pole, as illustrated in Fig.12. When rotating the rotor, i.e. changing angle θ from 0 to 90 degree, the torques have been calculated.

The results of the constant value β equal to 1, 3 and 5 are given in Fig.13. It can be seen that when a constant β is superimposed to the control current, the torque has almost no change, even if β is changed from 1 to 5, thus, it can be concluded that superimposing a constant to the control current will not interfere with the motor function.

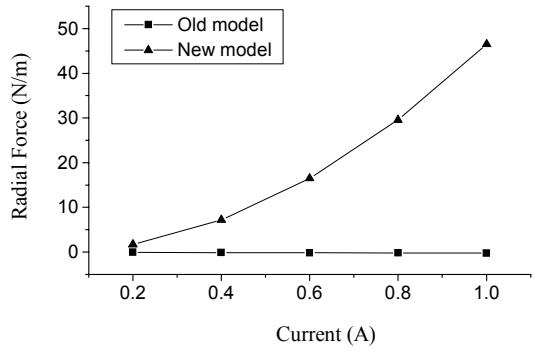

Fig.10 Radial force comparison for the new and old model

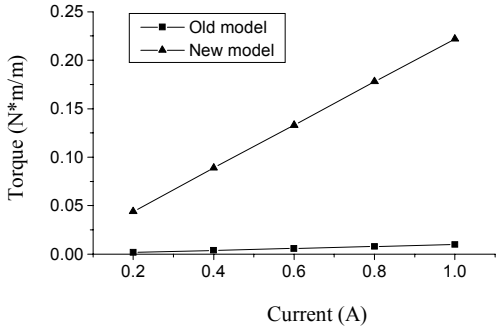

Fig.11 Torque comparison for new and old model

C. Control current arrangement for radial force

In order to find the radial force control current arrangement, a series of calculation has been carried out. The control current arrangement is shown in Fig.14. The radial forces and torque have been calculated corresponding to various rotor angular positions. The results are shown in Fig.15 and Fig.16.

When the radial force control current arrangement rotates 90 degree in counterclockwise, as shown in Fig.17, the radial forces and torque have also been calculated corresponding to rotor angular positions, and the results are shown in Fig.18 and Fig.19.

From Fig.15 and Fig.18, it can be seen that the specified radial forces are about ten times to lateral forces. As a result, the radial forces can be guaranteed by the control currents shown in Fig.14 and Fig.17. Fig.16 and Fig.19 show the torques when we applied the currents which generate the radial force. These values are negligible compared with Fig.13.

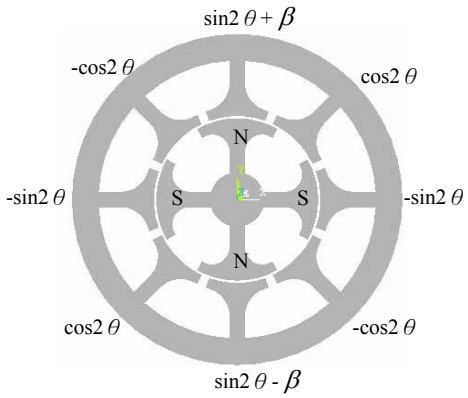

Fig.12 Control current arrangement

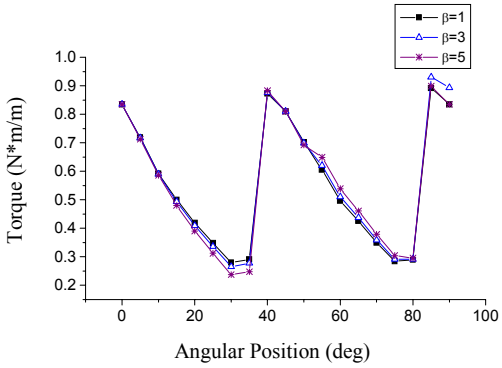

Fig.13 Torques versus superimposed rotor angular position

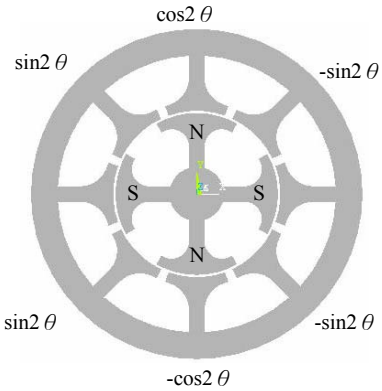

Fig.14 Control current arrangement for radial force (Fy)

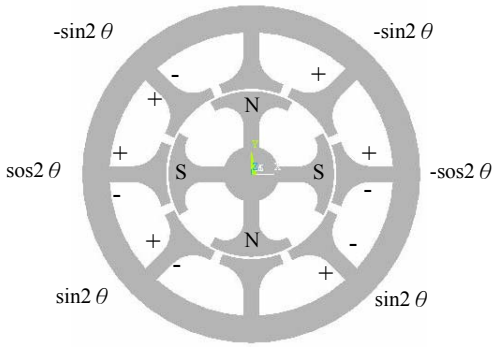

Fig.17 Radial force control current arrangement (*Fx*)

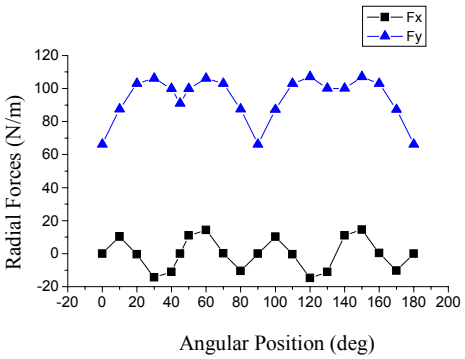

Fig.15 Radial force versus rotor angular position

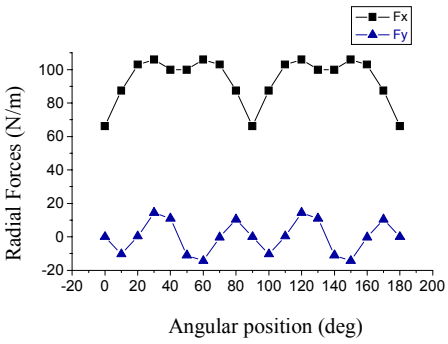

Fig.18 Radial force versus rotor angular position

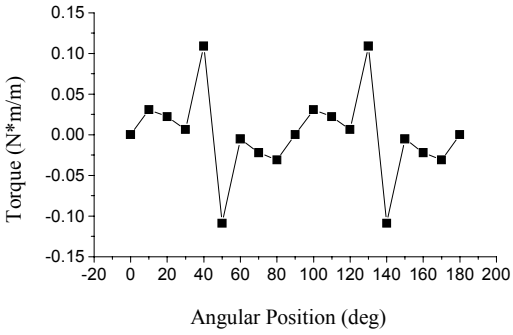

Fig.16 Torque versus rotor angular position

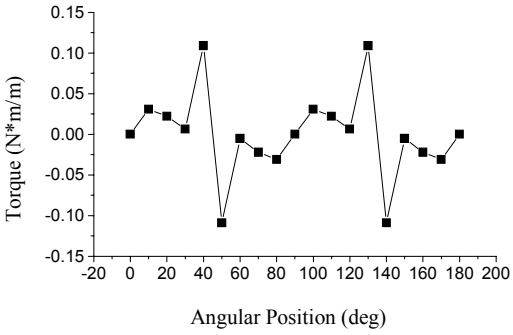

Fig.19 Torque versus rotor angular position

Therefore, the superimposition of the control current arrangement illustrated in Fig.6 and Fig.14 can be used to realize the rotor rotation and vertical radial force control, meanwhile the superimpositions of the control current arrangements illustrated in Fig.6 and Fig.17 can be used to control the rotor rotation and horizontal radial force.

For a bearingless motor, constant suspension forces are desired, while Fig.15 and Fig.18, show that the radial forces fluctuate with the rotor angular positions. This problem may be reduced by feedback control. Because feedback control is easy to realized in al linear system, the linearity of the input current and output force has been examined. The linearity is verified by changing constant *k* as shown in Fig.20, *k* is a multiplying constant to control currents. Changing the constant *k* from 0 to 1, with the incremental value being 0.2, the radial forces in *x* and *y* directions *Fx* and *Fy* as well as the torques have been calculated. All the results are shown in Fig.21. The radial forces in *y* direction versus the constant *k* are shown in Fig.22.

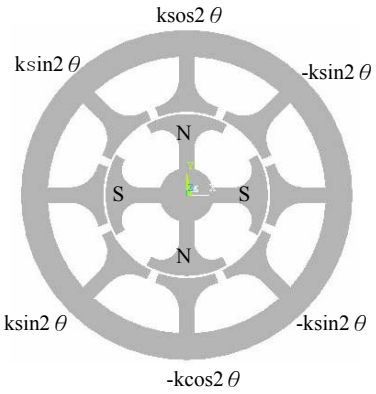

Fig.20 Radial force control current arrangement with constant *k*

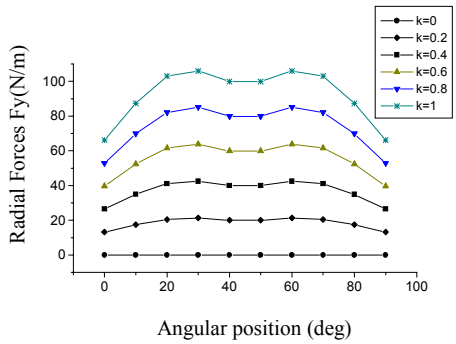

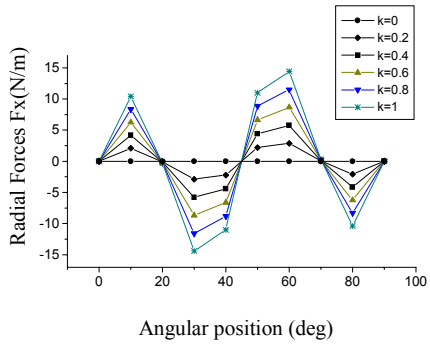

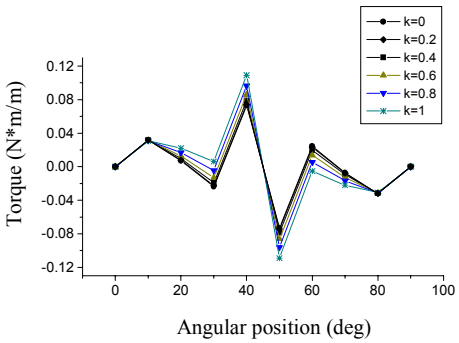

Fig.21 Force and torque with different constant *k*

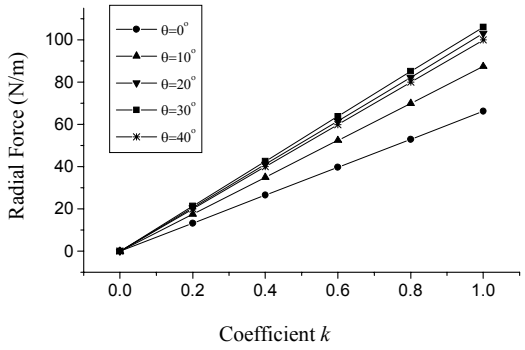

Fig.22 Radial force versus coefficient *k*

From Fig.22, it can be seen that the radial force and the coefficient *k* have a proportional relationship. That is the results verified that *k* and forces vary with linear relationship, feedback control can be adopted for levitation control.

IV CONCLUSIONS

FEM analyses and experimental results indicate that the proposed bearingless motor with rectifier circuits can be realized. For the improved bearingless motor dimensions, analysis results show that sufficient radial forces and torque can be generated, and the radial force and rotation torque control strategy has been determined primarily.

REFERENCES

[1] M. Takemoto, H. Suzuki and A. Chiba, "Improved analysis of a bearingless switched reluctance motor," IEEE Transaction on Industry Applications, vol.37, No.1, pp.26-34, January/February 2001.

[2] A. Chiba, Desmond T.Power, and M. Azizur Rahman, "Analysis of no-load characteristics of a bearingless induction motor," IEEE Transactions on industry applications, vol. 31, No.1, pp.77-83, January/February 1995.

[3] A. Chiba, M. Hanazawa, T, Fukao and M. Azizur Rahman, "Effects of magnetic saturation on radial force of bearingless synchronous reluctance motors," IEEE Transactions on industry applications, vol.32, No.2, pp.354-362, March/April, 1996.

[4] M. Oshima, S. Miyazawa, T. Deido and A. Chiba, "Characteristics of a permanent magnet type bearingless motor," IEEE Transactions on industry applications, vol.32, pp.363-370, March/April, 1996.

[5] Andres O. Salazar, A. Chiba and T. Fukao, "A review of developments in bearingless motors," 7th internation Symp. On magnetic bearings, pp.335-340, August, 2000

[6] W. Amrhein, S. Silber, K. Nenninger, G. Trauner and M. Reisinger, "Developments on bearingless drive technology," 8th international symposium on magnetic bearing. Mito, Japan pp.229-234, August, 2002.

[7] Koichi Oka, "Bearingless motor with rectifier circuits," 8th international symposium on magnetic bearing, Mito, Japan pp.271-275, August, 2002.